



Available online at www.sciencedirect.com

SCIENCE @ DIRECT®

C. R. Chimie 9 (2006) 639–644



<http://france.elsevier.com/direct/CRAS2C/>

Preliminary communication / Communication

Effect of excitation wavelength on electron injection efficiency in dye-sensitized nanocrystalline TiO₂ and ZrO₂ films

Ryuzi Katoh *, Akihiro Furube, Miki Murai, Yoshiaki Tamaki,
Kohjiro Hara, M. Tachiya

National Institute of Advanced Industrial Science and Technology (AIST), AIST Tsukuba Central 5, Tsukuba, Ibaraki 305-8565, Japan

Received 20 September 2004; accepted after revision 11 April 2005

Available online 19 September 2005

Abstract

The effect of excitation wavelength on the efficiency of electron injection from N3 dye (*cis*-bis(4,4'-dicarboxy-2,2'-bipyridine)di(thiocyanato)ruthenium(II); Ru(dcbpy)₂(NCS)₂) to nanocrystalline TiO₂ and ZrO₂ films was studied by transient absorption spectroscopy. For TiO₂ films, electron injection occurred efficiently (> 80 %), and the efficiency did not depend on excitation wavelength. For ZrO₂ films, no electron injection was observed even with shorter-wavelength excitation in a polar solvent. **To cite this article:** R. Katoh *et al.*, *C. R. Chimie* 9 (2006).

© 2005 Académie des sciences. Published by Elsevier SAS. All rights reserved.

Résumé

L'effet de la longueur d'onde d'excitation sur l'efficacité de l'injection d'électrons à partir du pigment N3 (*cis*-bis(4,4'-dicarboxy-2,2'-bipyridine) di(thiocyanato)ruthénium(II) ; Ru(dcbpy)₂(NCS)₂) vers des films nanocristallins de TiO₂ et de ZrO₂ a été étudié par spectroscopie d'absorption transitoire. Pour les films de TiO₂, l'injection d'électrons s'est faite avec une bonne efficacité (> 80%), indépendante de la longueur d'onde d'excitation. Pour les films de ZrO₂, aucune injection d'électrons n'a été observée, même avec une excitation de longueur d'onde plus courte dans un solvant polaire. **Pour citer cet article :** R. Katoh *et al.*, *C. R. Chimie* 9 (2006).

© 2005 Académie des sciences. Published by Elsevier SAS. All rights reserved.

Keywords: Dye-sensitized nanocrystalline TiO₂ and ZrO₂ films; Transient absorption spectroscopy

Mots clés : Films nanocristallins TiO₂ et ZrO₂ sensibilisés par pigments ; Spectroscopie d'absorption transitoire

* Corresponding author.

E-mail address: r-katoh@aist.go.jp (R. Katoh).

1. Introduction

Since highly efficient dye-sensitized solar cells were first reported [1], much research has been carried out to achieve higher performance. For this purpose, the primary processes of dye-sensitized solar cells have been studied extensively. Dye-sensitized solar cells are a kind of photoelectrochemical cell [2]. To realize a high light-harvesting efficiency in the visible wavelength range, nanocrystalline semiconductor films are used as electrodes, and sensitizer dyes are tightly chemically bound to the surface of the semiconductor. Upon photoexcitation by visible wavelength light, electron injection from the excited dye to the semiconductor film occurs efficiently. Electron injection is the first, and most important, primary process in dye-sensitized solar cells.

We [3–9] and others [10–22] have extensively used transient absorption spectroscopy to study electron injection processes. The dynamics of electron injection has been studied by femtosecond laser spectroscopy, and electron injection has been found to complete within 10 ps [15–20]. This is much faster than the excited state lifetime of typical sensitizer dyes, and therefore the efficiency of electron injection is expected to be very high if there are no other ultrafast relaxation channels from the excited state to the ground state. Thus, to discuss the injection process quantitatively, it is necessary to directly estimate quantitatively the efficiency of electron injection.

Because it is difficult to estimate the number of transient species in transient absorption spectroscopy, there have been only a few attempts to evaluate the efficiency quantitatively. Recently, we quantitatively estimated the efficiency for N3 dye (*cis*-bis(4,4'-dicarboxy-2,2'-bipyridine)di(thiocyanato)ruthenium(II); Ru(dcbpy)₂(NCS)₂) adsorbed on a nanocrystalline TiO₂ film (abbreviated N3/TiO₂); the estimated efficiency was 95% under 532-nm excitation [6]. The efficiency of electron injection is sensitive to experimental conditions, such as excitation light intensity [7] and concentration of Li⁺ [11,12].

To achieve high performance in dye-sensitized solar cells, the absorption spectrum of the sensitizer dye must be wide in the visible wavelength range. Moreover, the photon-to-electron conversion efficiency must be high over this wavelength range. Thus, the effect of the excitation wavelength on the electron injection process is a

very important parameter for understanding the primary process and for creating a strategy for developing highly efficient solar cells. The effect of excitation wavelength on the electron injection dynamics has been studied by Durrant's group [15,16], Sundström's group [19], and Lian's group [17,18]. Moser et al. [13] studied the effect of wavelength on the efficiency by analyzing transient absorption signals in the nanosecond time range. Although the wavelength dependence reported by these groups is very important in discussing the primary processes, it is difficult to discuss the injection process quantitatively without directly evaluating the efficiency of electron injection, as mentioned above.

Fig. 1 shows the energy level diagram for electron injection from the N3 dye to the semiconductor. The energy levels are shown with respect to the energy of the oxidation potential (N3/N3⁺) of the N3 dye in the ground state. The absorption spectrum of the N3 dye is shown on the right-hand side of the figure. In the lower energy range, the transition to the lowest singlet metal-to-ligand charge-transfer state (¹MLCT) is observed, and the peak appears at around 530 nm (2.34 eV). The transition to the higher ¹MLCT (¹MLCT*) state be-

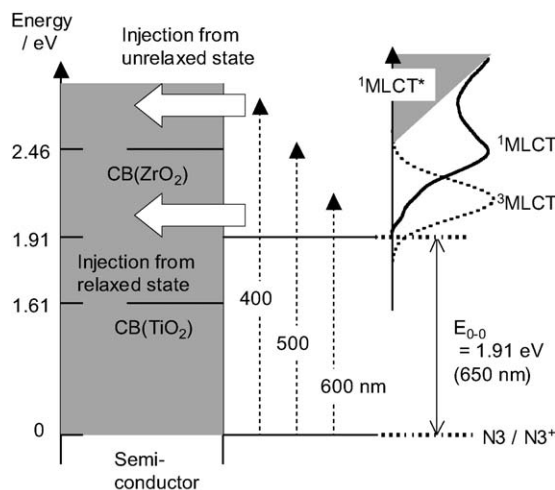


Fig. 1. Energy-level diagram for electron injection from an excited N3 dye to a semiconductor film with respect to the oxidation potential of the N3 dye in the ground state. The energy levels of the ¹MLCT and ¹MLCT* states (absorption spectrum) and the ³MLCT state estimated from the fluorescence spectrum are shown. The energies of the conduction band edges of TiO₂ and ZrO₂ are shown on the left-hand side. Electron injection occurs from the higher excited state, reached by optical absorption before and after relaxation, to the lowest excited state.

comes pronounced in the higher energy range (> 2.5 eV) [23]. Intersystem crossing from the singlet MLCT state to the triplet MLCT ($^3\text{MLCT}$) state of the N3 dye is very fast (< 100 fs [19]), and therefore the $^3\text{MLCT}$ state is populated immediately. In Fig. 1, the energy position of $^3\text{MLCT}$ estimated from the fluorescence spectrum of N3 dye is schematically indicated. Excitation wavelengths are also shown by the arrows. The energy levels of the conduction band edges of ZrO_2 (2.46 eV) and TiO_2 (1.61 eV) are indicated. For N3/ TiO_2 , Sundström et al. reported that the excited state produced by photoexcitation can inject electrons into the semiconductor before and after relaxation to $^3\text{MLCT}$ [19]. For N3/ ZrO_2 , electron injection was observed with shorter-wavelength light (< 520 nm) in polar solvents [22].

To discuss the injection process quantitatively, we studied here the effect of excitation wavelength on the efficiency of electron injection in N3/ TiO_2 and N3/ ZrO_2 films through transient absorption measurements.

2. Experimental

TiO_2 nanoparticles were prepared by the method reported by Barbé et al. [24]. For ZrO_2 , commercially available powders (Sumitomo Osaka Cement Co. Ltd.) were used. An organic paste containing the semiconductor nanoparticles was printed onto a glass substrate by a screen-printing technique [25]. The films obtained had an area of 1 cm^2 ($1\text{ cm} \times 1\text{ cm}$) and a thickness of $2\text{--}5\text{ }\mu\text{m}$. The N3 dye (Solaronix SA) was used without purification and was dissolved in a 50:50 solution of *tert*-butyl alcohol (Kanto Chemical) and acetonitrile (Kanto Chemical, dehydrated) to give a 0.3 mM solution. The semiconductor films were immersed in the dye solution and then kept at $25\text{ }^\circ\text{C}$ for at least 10 h so that the dye could be adsorbed onto the semiconductor surface. The sample specimens were dried in air and used for transient absorption measurements. All measurements were carried out just after the preparation of the sample specimens to minimize the effect of dye degradation.

Absorption spectra were measured with an absorption spectrophotometer (Shimadzu, UV-3101PC). Light transmitted through a sample specimen was corrected by an integrating sphere to minimize artifacts due to light scattering by the substrate. For the transient absorption measurements, light pulses from an optical

parametric oscillator (OPO) system (Spectra Physics, MOPO-SL) excited by a Nd^{3+} :YAG laser (Spectra Physics, Pro-230-10) were used for pumping light. The duration of the laser pulse was about 10 ns. A Xe flash lamp (Hamamatsu, L4642, $2\text{-}\mu\text{s}$ pulse duration) was used as a probe light source. The probe light was focused on a sample specimen (2 mm in diameter). The area probed by the probe light was covered by that irradiated with the exciting light (10 mm in diameter). The probe light transmitted through the sample specimen was detected with a Si photodiode (Hamamatsu, S-1722) after being dispersed with a monochromator (Ritsu, MC-10N). Signals from the photodetector were processed with a digital oscilloscope (Tektronix, TDS680C) and were analyzed with a computer. The intensity of the laser pulse was measured with a pyroelectric energy meter (Ophir, PE25-SH-V2). All measurements were carried out at 295 K .

3. Results and discussion

Fig. 2 shows transient absorption spectra of N3/ TiO_2 and N3/ ZrO_2 films excited with 532-nm light. For N3/ TiO_2 , a peak at 780 nm was observed and was assigned to the oxidized form of N3 dye [7,15]. For N3/ ZrO_2 , on the contrary, there is no peak around 780 nm , but a peak at 680 nm can be seen. This peak was assigned to the absorption band due to the $^3\text{MLCT}$ state of N3 dye on the basis of the similarity of the absorption spectrum of N3 dye in solution [15]. This indicates that no electron injection occurs. This is rea-

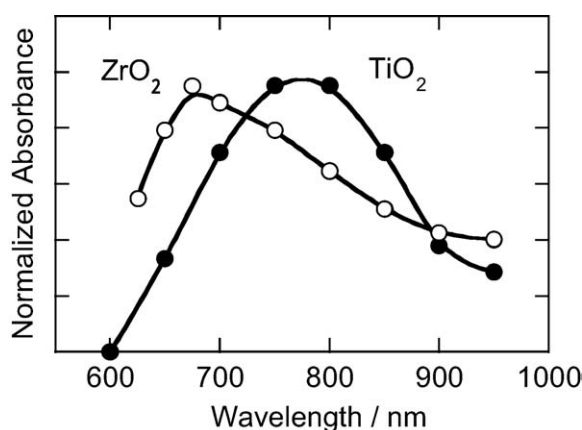


Fig. 2. Transient absorption spectra of N3/ TiO_2 and N3/ ZrO_2 excited with 532-nm light pulses.

sonable because the energy level reached by 532-nm light absorption is 2.33 eV, which is lower than the energy level of the conduction band edge of ZrO_2 (2.46 eV).

Fig. 3 shows the temporal profile of the transient absorption signal of N3/TiO₂ observed at 800 nm with 532-nm excitation. The signal rises immediately after excitation, and no decay in this time range can be seen. These results clearly show that the electron injection is very fast and the recombination is slow, which is consistent with previous observations [7]. We already estimated the absorption coefficient of the oxidized form (N3⁺) of N3 dye as 6000 mol⁻¹ dm³ cm⁻¹ [6]; therefore the efficiency of electron injection can be estimated quantitatively from the observed absorbance change. Fig. 4 shows the absorbance change of N3/TiO₂ at 800 nm as a function of excitation intensity of 450-, 550-, and 650-nm light. The absorbance changes are proportional to the excitation light intensity. Under this condition, the efficiency of electron injection Φ_{inj} can be written in terms of the absorbance change due to the generation of N3⁺ (ΔA_{ox}) and the molar absorption coefficient ϵ_{ox} of N3⁺ [6]:

$$\Phi_{\text{inj}} = \frac{\Delta A_{\text{ox}}}{\epsilon_{\text{ox}} (1 - T) N_0} \quad (1)$$

where T and N_0 represent the transmittance of excitation light and the number of incident excitation photons per unit area, respectively.

Fig. 5 shows the efficiency of electron injection in N3/TiO₂ as a function of excitation wavelength. The efficiencies are very high (> 80%) and do not depend

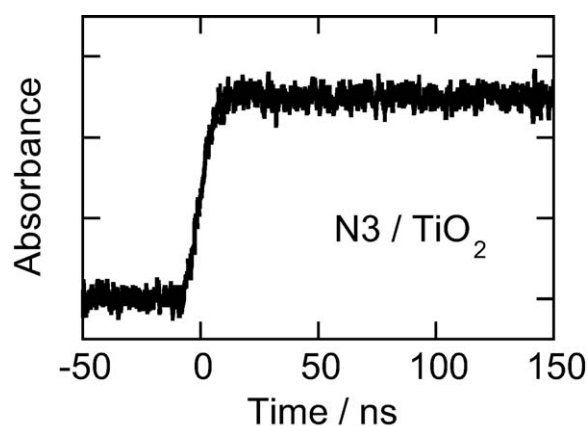


Fig. 3. Temporal profile of transient absorption of N3/TiO₂ observed at 800 nm. Excitation wavelength, 532 nm.

on the excitation wavelength. A similar tendency was reported by Moser et al. [13] from the analysis of transient absorption signals. The absorption spectrum of the film is also shown in Fig. 5. The peak at 520 nm is assigned to the transition to the lowest singlet metal-to-ligand charge-transfer (¹MLCT) state, and the transition to a higher MLCT (¹MLCT*) state is pronounced at shorter-wavelengths. Specifically, the final (Franck–Condon) state of optical transition is different among the excitation wavelengths. When the excitation wavelength is longer than 500 nm, the ¹MLCT state

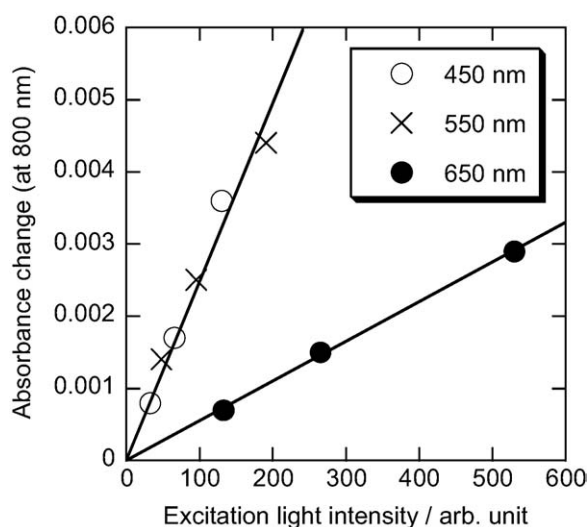


Fig. 4. Absorbance change of N3/TiO₂ at 800 nm as a function of excitation intensity. Excitation wavelengths: 450, 550, and 650 nm.

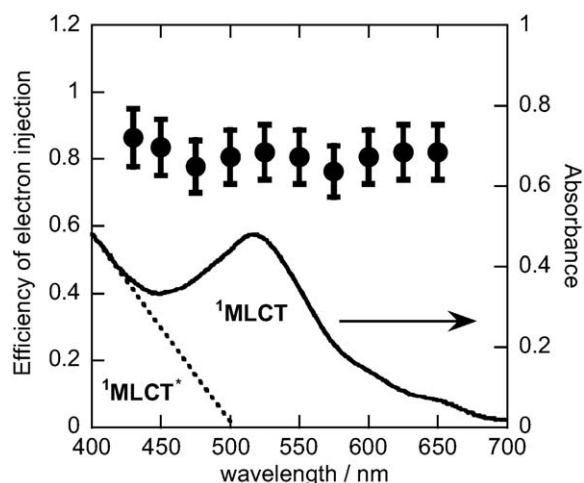


Fig. 5. Efficiency of electron injection of N3/TiO₂ as a function of excitation wavelength. The absorption spectrum is also shown.

is mainly populated. For shorter-wavelength excitation (< 500 nm), the contribution of $^1\text{MLCT}^*$ increases with decreasing excitation wavelength. The difference of the final state of the optical transition does not seem to affect the efficiency of electron injection. This implies that all excited states of the N3 dye can inject electrons efficiently.

The dynamics of ultrafast electron injection has been studied [15–20]. For N3/TiO₂, very fast injection (<100 fs) and slower injection (<10 ps) were observed. It has been reported that the fast process is due to electron injection from the unrelaxed Franck–Condon state ($^1\text{MLCT}$ and $^1\text{MLCT}^*$) [19] and that the slower process is due to injection from the relaxed state ($^3\text{MLCT}$). Durrant et al. [16] studied the effect of excitation wavelength on the injection dynamics and observed similar dynamics with 520-, 560-, and 600-nm excitation. Sundström and co-workers observed a remarkable difference in the dynamics between 530 and 455-nm excitation [19]. They observed that the faster process was pronounced with 455-nm excitation. Lian and co-workers measured the injection dynamics with 400-, 530-, and 630-nm excitation and also observed that the faster process was pronounced with shorter-wavelength excitation [18]. These reports clearly show that the injection dynamics changes with changing wavelength. With shorter-wavelength excitation (< 500 nm), the very fast injection from the unrelaxed state occurs efficiently. This implies that the higher excited MLCT ($^1\text{MLCT}^*$) state populated by shorter-wavelength light (< 500 nm) can inject electrons effectively, suggesting that the $^1\text{MLCT}^*$ state has a large electronic coupling for the electron injection. As we observed, the efficiency of electron injection is not sensitive to the excitation wavelength (Fig. 5). This finding indicates that after relaxation to the $^3\text{MLCT}$ state, electron injection still occurs efficiently and that there are no other direct relaxation channels from the higher excited MLCT ($^1\text{MLCT}^*$) state to the ground state.

Heimer et al. [14] reported the absorbed-photon-to-current conversion efficiency (APCE) of solar cells based on the N3/TiO₂ electrode. They observed that the APCE decreases for wavelengths of 600–700 nm, whereas the efficiency of electron injection is constant (Fig. 5). The discrepancy may be due to some other factors in solar cells, for instance absorption of excitation light by reaction intermediates in working solar cells.

As shown in Fig. 2, electron injection does not occur in N3/ZrO₂ with 532-nm excitation. The energy of the conduction band edge of ZrO₂ is located at 2.46 eV with respect to the oxidation potential of N3 dye. This is higher than the energy level of the $^3\text{MLCT}$ state of N3 dye (1.91 eV) and the photon energy of 532-nm light (2.33 eV). Thus, no electron injection is expected. As mentioned above, electron injection from the unrelaxed state has been observed in N3/TiO₂. Thus, it may be possible that electron injection occurs from the unrelaxed state in N3/ZrO₂ with shorter-wavelength (< 500 nm) excitation.

Fig. 6 shows the decay profile of the transient absorption signal in N3/ZrO₂ observed at 800 nm under various conditions. Traces a and b are the decay profiles with 530 and 430-nm excitation, respectively, and trace c is the decay profile with 430-nm excitation in acetonitrile. There are no significant differences between the traces except that the decay of trace c is slightly longer than the decays of traces a and b. These decay rates are similar to emission decay rates [7,15]. We also measured transient absorption spectra under these conditions; the spectra are similar to the spectrum shown in Fig. 2. These results clearly indicate that electron injection

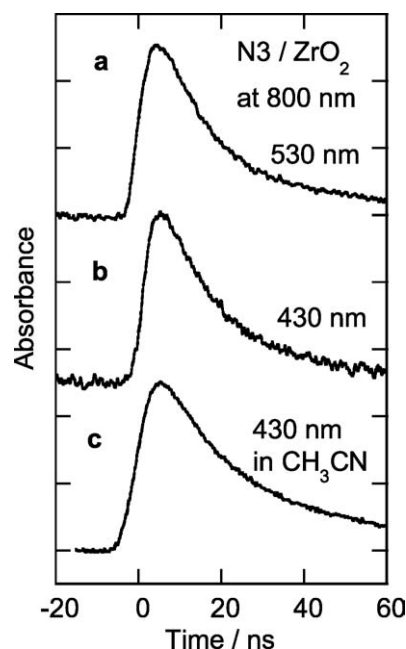


Fig. 6. Temporal profiles of transient absorption of N3/ZrO₂ observed at 800 nm: (a) excitation wavelength, 530 nm; (b) excitation wavelength, 430 nm; (c) excitation wavelength, 430 nm; acetonitrile solvent.

tion from the unrelaxed excited state of N3 dye to the conduction band of ZrO_2 is not efficient.

Kelly and co-workers reported that electron injection occurs from N3 dye to TiO_2 colloid in polar solvents with 519- and 495-nm excitation and that no injection occurs with 630-nm excitation [22]. As mentioned above, we observed no electron injection in N3/ ZrO_2 . This discrepancy may be due to the time scale difference of these observations; that is, the studies of Kelly et al. were carried out in the picosecond time range, whereas our studies were performed in the nanosecond time range. Electron injection is not necessarily detected in the nanosecond time range if a very fast recombination process occurs efficiently. Huber et al. studied electron injection from a strong coupled sensitizer dye to ZrO_2 and observed fast recombination in the picosecond time range [21]. Huber et al. explained this fast recombination in the ZrO_2 system by the recombination between a parent cation and a partially injected electron; that is, an electron trapped in the surface state of ZrO_2 . Thus, in the present study, a similar process may occur; namely, electron injection occurs from the excited N3 dye to the surface state of ZrO_2 and not to the conduction band of ZrO_2 under our excitation conditions. The role of the surface state in the electron injection process is not fully understood. Recently, we reported the electron injection dynamics in an organic dye coupled with surface states [9].

Acknowledgements

This work was supported by the COE development program, and by Grant-in-Aid for Scientific Research from the Ministry of Education, Culture, Sports, Science and Technology (MEXT) of Japan.

References

- [1] M.K. Nazeeruddin, A. Kay, I. Rodicio, R. Humphry-Baker, E. Müller, P. Liska, N. Vlachopoulos, M. Grätzel, *J. Am. Chem. Soc.* 115 (1993) 6382.
- [2] A. Hagfeldt, M. Grätzel, *Chem. Rev.* 95 (1995) 49.
- [3] K. Hara, H. Horiuchi, R. Katoh, L.P. Singh, H. Sugihara, K. Sayama, S. Murata, M. Tachiya, H. Arakawa, *J. Phys. Chem. B* 106 (2002) 374.
- [4] H. Horiuchi, R. Katoh, K. Hara, M. Yanagida, S. Murata, H. Sugihara, H. Arakawa, M. Tachiya, *J. Chem. Phys. B* 107 (2003) 2570.
- [5] R. Katoh, A. Furube, K. Hara, S. Murata, H. Sugihara, H. Arakawa, M. Tachiya, *J. Phys. Chem. B* 106 (2002) 12957.
- [6] T. Yoshihara, R. Katoh, A. Furube, M. Murai, T. Tamaki, K. Hara, S. Murata, H. Arakawa, M. Tachiya, *J. Phys. Chem. B* 108 (2004) 2643.
- [7] R. Katoh, A. Furube, T. Yoshihara, K. Hara, G. Fujihashi, S. Takano, S. Murata, H. Arakawa, M. Tachiya, *J. Phys. Chem. B* 108 (2004) 4818.
- [8] A. Furube, R. Katoh, K. Hara, S. Murata, H. Arakawa, M. Tachiya, *J. Phys. Chem. B* 107 (2003) 4162.
- [9] A. Furube, R. Katoh, T. Yoshihara, K. Hara, S. Murata, H. Arakawa, M. Tachiya, *J. Phys. Chem. B* 108 (2004) 12583.
- [10] S.A. Haque, Y. Tachibana, R.L. Willis, J.E. Moser, M. Grätzel, D.R. Klug, J.R. Durrant, *J. Phys. Chem. B* 104 (2000) 538.
- [11] C.A. Kelly, G.J. Meyer, *Coord. Chem. Rev.* 21 (2001) 295.
- [12] B.V. Bergeron, C.A. Kelly, G.J. Meyer, *Langmuir* 19 (2003) 8389.
- [13] J.E. Moser, M. Wolf, F. Lenzmann, M. Grätzel, *Z. Phys. Chem.* 212 (1999) 85.
- [14] T.A. Heimer, E.J. Heilweil, C.A. Bignozzi, G.J. Meyer, *J. Phys. Chem. A* 104 (2000) 4256.
- [15] Y. Tachibana, J.E. Moser, M. Grätzel, D.R. Klug, J.R. Durrant, *J. Phys. Chem.* 100 (1996) 20056.
- [16] J.R. Durrant, Y. Tachibana, I. Mercer, J.E. Moser, M. Grätzel, D.R. Klug, *Z. Phys. Chem.* 212 (1999) 93.
- [17] J.B. Asbury, E. Hao, Y. Wang, H.N. Ghosh, T. Lian, *J. Phys. Chem. B* 105 (2001) 4545.
- [18] J.B. Asbury, N.A. Anderson, E. Hao, X. Ai, T. Lian, *J. Phys. Chem. B* 107 (2003) 7376.
- [19] G. Benkő, J. Kalioinen, J.E.I. Korppi-Tommola, A.P. Yartsev, V. Sundström, *J. Am. Chem. Soc.* 124 (2002) 489.
- [20] C. Bauer, E. Boschloo, E. Mukhtar, A. Hagfeldt, *J. Phys. Chem. B* 105 (2001) 5585.
- [21] R. Huber, S. Spörlein, J.E. Moser, M. Grätzel, *J. Wachtveitl, J. Phys. Chem. B* 104 (2000) 8995.
- [22] C.M. Olsen, M.R. Waterland, D.F. Kelly, *J. Phys. Chem. B* 106 (2002) 6211.
- [23] M.K. Nazeeruddin, S.M. Zakeeruddin, R. Humphry-Baker, M. Jirousek, P. Liska, N. Vlachopoulos, V. Shklover, C.-H. Fischer, M. Grätzel, *Inorg. Chem.* 38 (1999) 6298.
- [24] C.J. Barbé, F. Arendse, P. Comte, M. Jirousek, F. Lenzmann, V. Shklover, M. Grätzel, *J. Am. Ceram. Soc.* 80 (1997) 3157.
- [25] K. Hara, T. Horiguchi, T. Kinoshita, K. Sayama, H. Sugihara, H. Arakawa, *Sol. Energy Mater. Sol. Cells* 64 (2000) 115.